The Signature of the Western Boundary Currents on Tropospheric Variability

James Larson[1], David W. J. Thompson[1], James W. Hurrell[1]

[1]Department of Atmospheric Science, Colorado State University

NCAR CVCWG March 2024

Image credit to NOAA

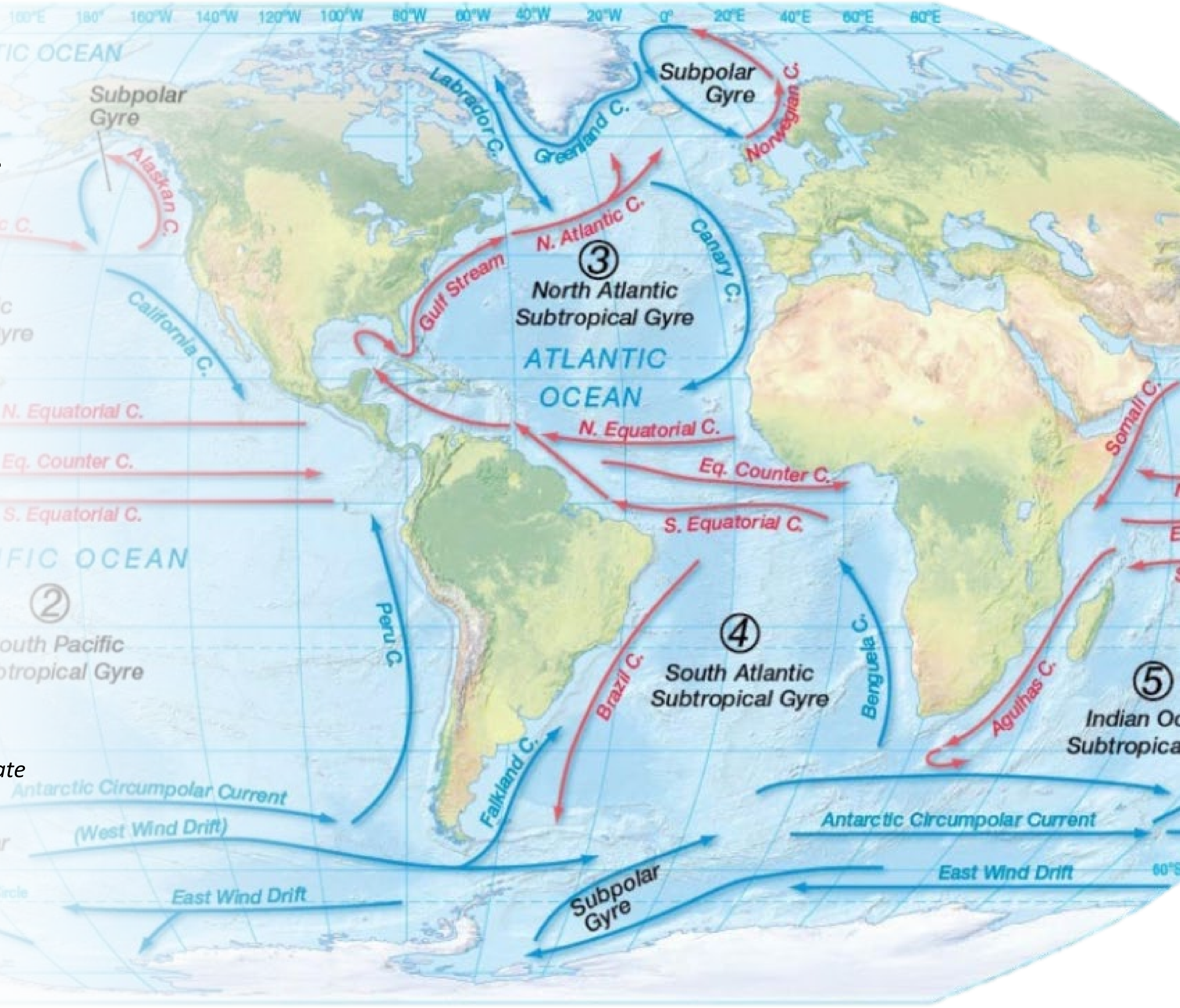

It is clear that western boundary currents influence the **time-mean** tropospheric climate

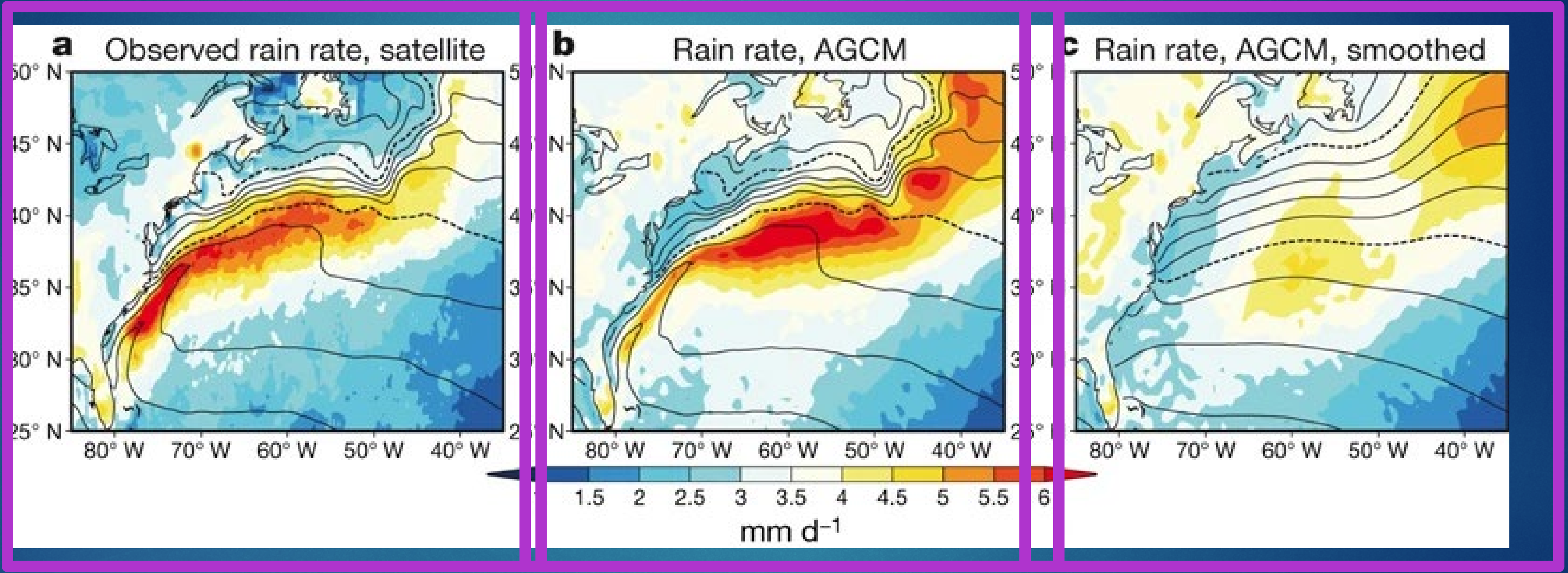

1. Minobe, Shoshiro, Akira Kuwano-Yoshida, Nobumasa Komori, Shang-Ping Xie, and Richard Justin Small. "Influence of the Gulf Stream on the Troposphere." Nature 452, no. 7184 (March 2008): 206–9. https://doi.org/10.1038/nature06690.

It is less clear how variations in midlatitude sea surface temperatures (SST) influence tropospheric **variability**

Do aspects of the troposphere(such as vertical motion, precipitation, etc.) co-vary with SST anomalies over western boundary currents?

Data and Methodology

- ECMWF Reanalysis v5 (**ERA5**)[3]
  - Time period of interest: September **2007** – December **2022**
  - Horizontal resolution: 1/4° (~25km)
- iHESP experiments[5] - **CESM v1.3**[6] - **Fully coupled**
  - "**Low**-resolution" – **1°** horizontal resolution for both atmosphere and ocean
  - "**High**-resolution" – **1/10° resolution for ocean** and 1/4° for atmosphere
  - 250 years of **pre-industrial control** forcings
- All results are based on **monthly-mean anomalies**
- All results are for extended **wintertime**
  - ONDJFM (AMJJAS) for Northern (Southern) Hemisphere

[3] Hersbach et al. (2020) [5] Chang et al. (2020) [6] Hurrell et al. (2013)

Strong time-mean vertical motion and precipitation exists on the warm side of ∇SST

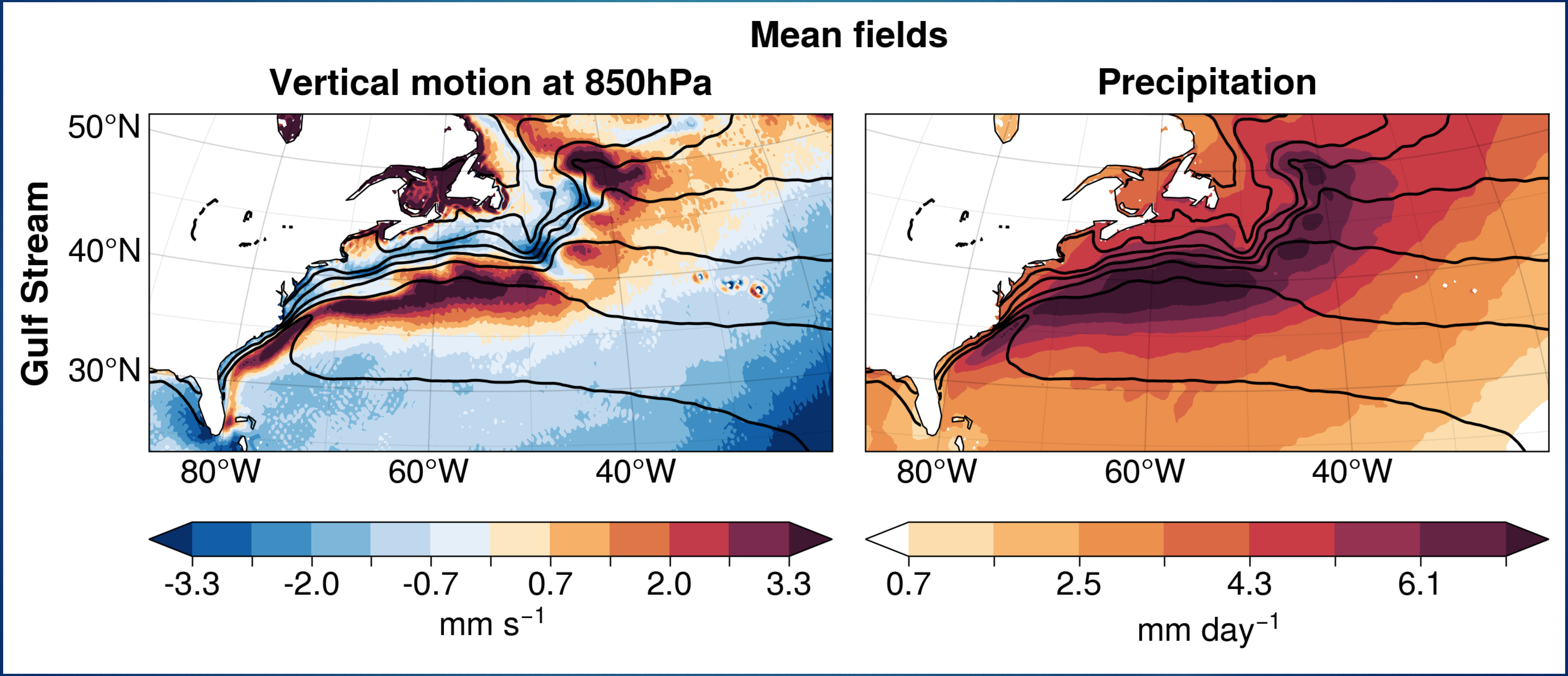

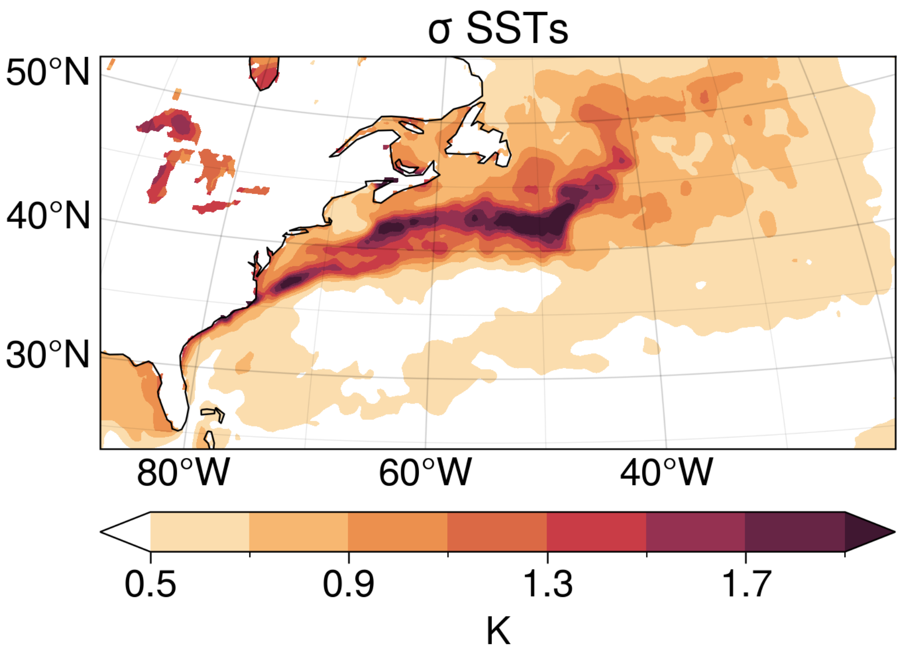

Regression as a function of grid cells highlights the signature of the Gulf Stream on the atmosphere

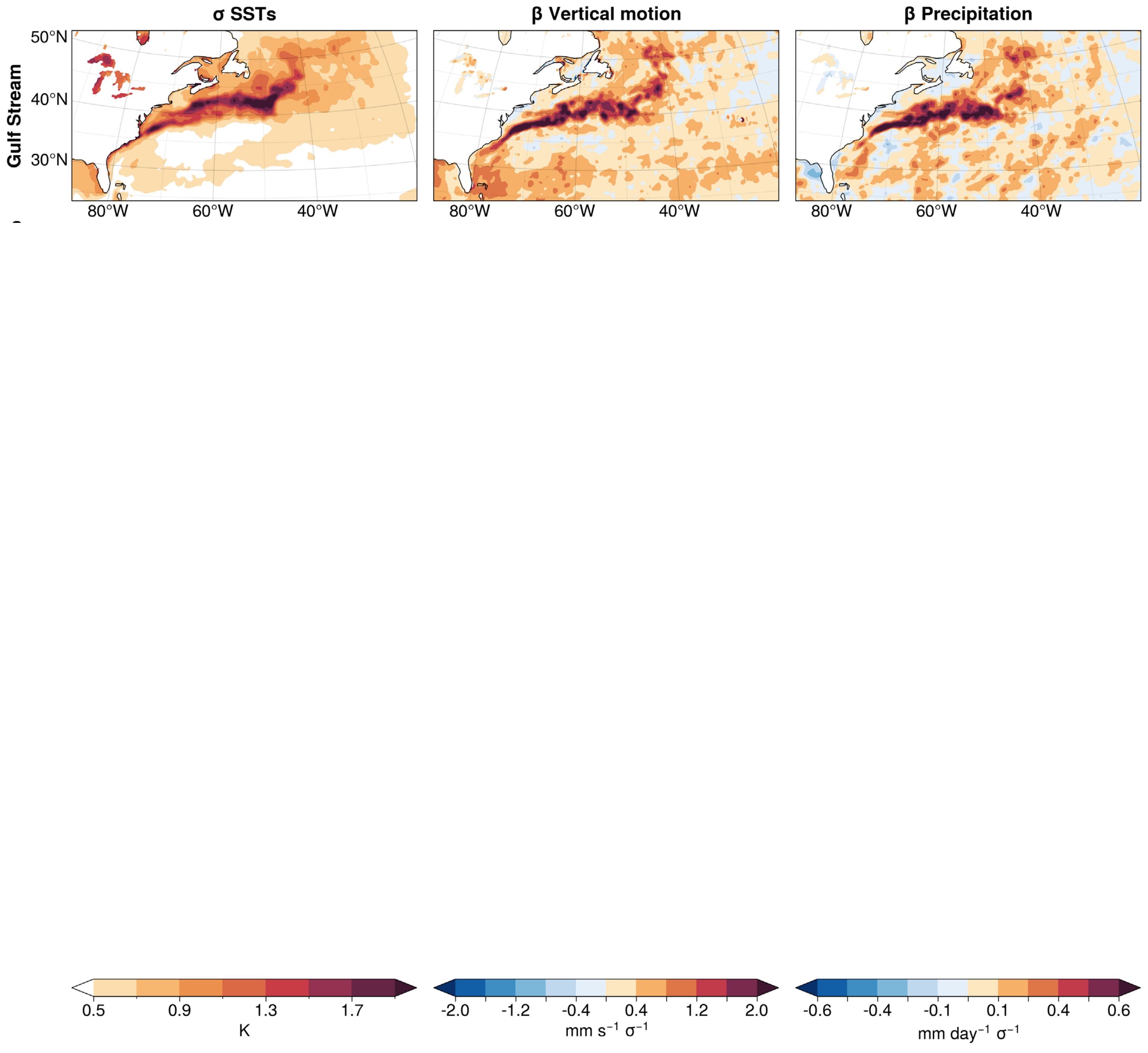

The world's five strongest western boundary currents all leave signatures on local circulation

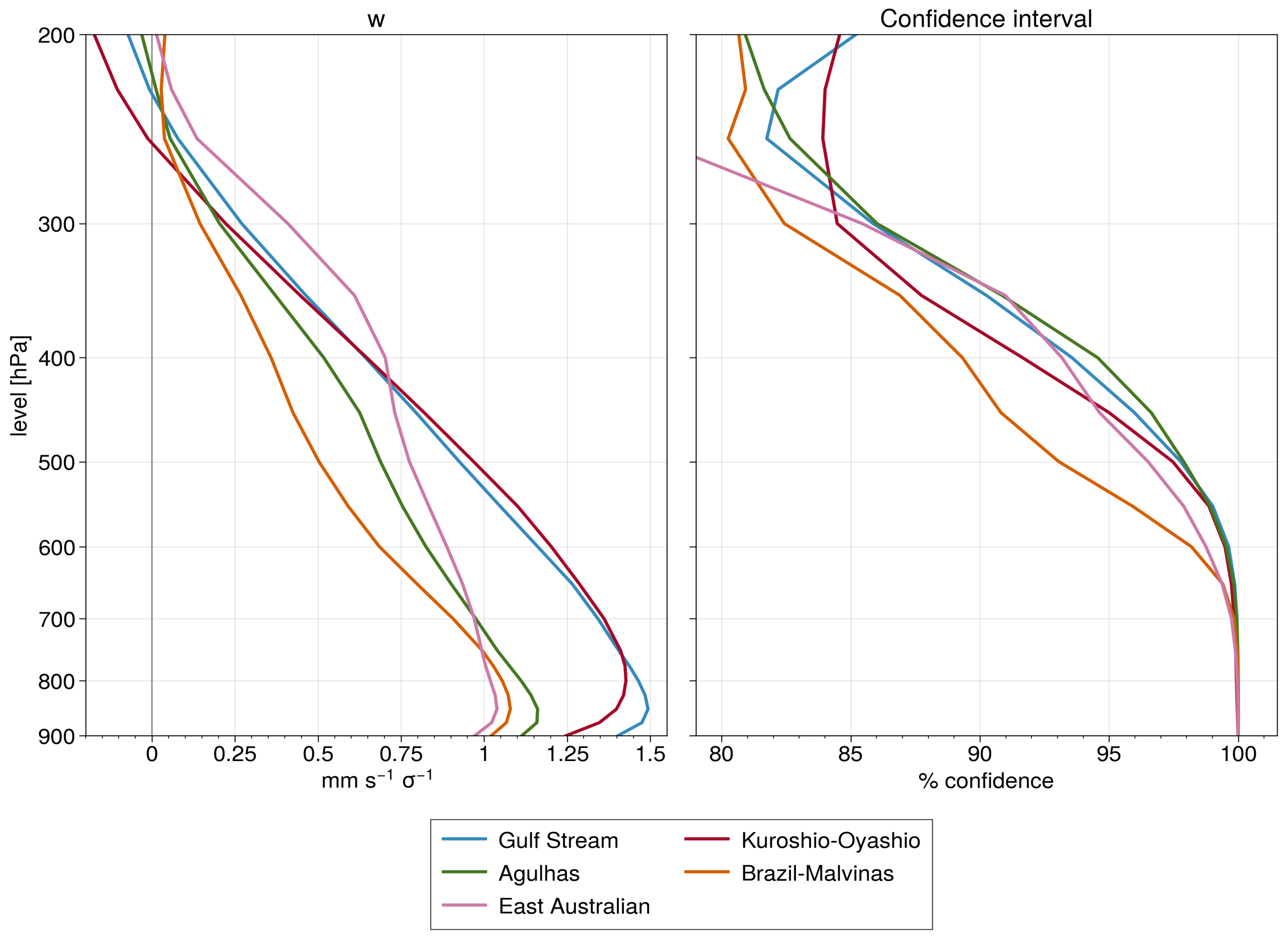

Vertical motion is found to co-vary with SST anomalies into at least the middle troposphere

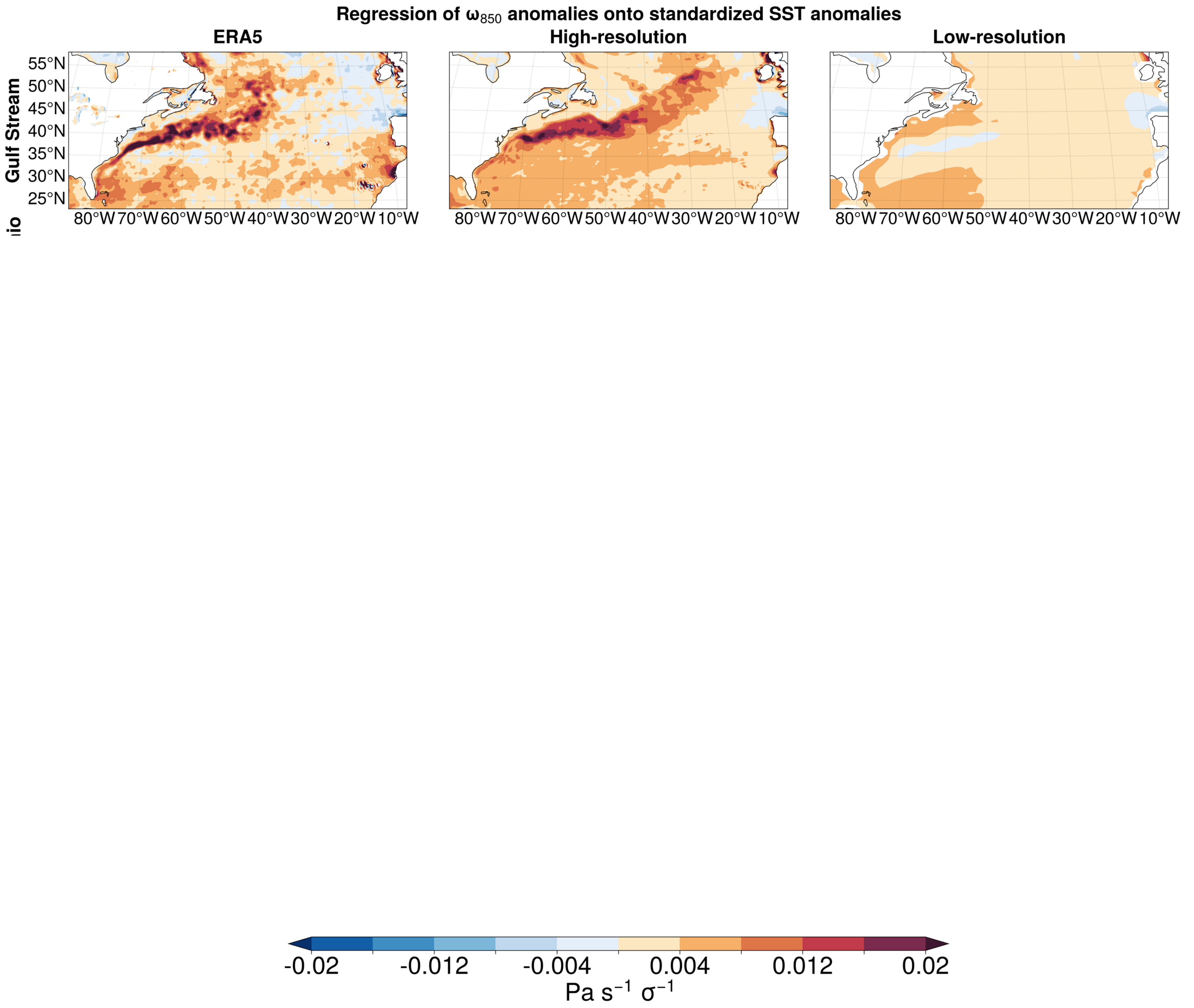

High-spatial-resolution is necessary to capture this air-sea co-variability in CESM

Conclusion

- **Establishes co-variability between SST anomalies and local atmospheric changes** over western boundary currents
- **Consistent air-sea co-variability** is found over **five** of the strongest **western boundary currents**
- Highlights that **western boundary currents are a uniquely separate regime** for midlatitude air-sea co-variability relative to the internal ocean basins
- Future work aims to look at the signature of the western boundary currents on the variability of clouds, radiation, and global circulations

Thank you! Please feel free to reach out at james.larson@colostate.edu

Supplementary

References

1. Chelton, Dudley B., Michael G. Schlax, Michael H. Freilich, and Ralph F. Milliff. "Satellite Measurements Reveal Persistent Small-Scale Features in Ocean Winds." Science 303, no. 5660 (February 13, 2004): 978–83. https://doi.org/10.1126/science.1091901.
2. Minobe, Shoshiro, Akira Kuwano-Yoshida, Nobumasa Komori, Shang-Ping Xie, and Richard Justin Small. "Influence of the Gulf Stream on the Troposphere." Nature 452, no. 7184 (March 2008): 206–9. https://doi.org/10.1038/nature06690.
3. Hersbach, Hans, Bill Bell, Paul Berrisford, Shoji Hirahara, András Horányi, Joaquín Muñoz-Sabater, Julien Nicolas, et al. "The ERA5 Global Reanalysis." Quarterly Journal of the Royal Meteorological Society 146, no. 730 (July 2020): 1999–2049. https://doi.org/10.1002/qj.3803.
4. Donlon, Craig J., Matthew Martin, John Stark, Jonah Roberts-Jones, Emma Fiedler, and Werenfrid Wimmer. "The Operational Sea Surface Temperature and Sea Ice Analysis (OSTIA) System." Remote Sensing of Environment 116 (January 2012): 140–58. https://doi.org/10.1016/j.rse.2010.10.017.
5. Chang, Ping, Shaoqing Zhang, Gokhan Danabasoglu, Stephen G. Yeager, Haohuan Fu, Hong Wang, Frederic S. Castruccio, et al. "An Unprecedented Set of High-Resolution Earth System Simulations for Understanding Multiscale Interactions in Climate Variability and Change." Journal of Advances in Modeling Earth Systems 12, no. 12 (December 2020). https://doi.org/10.1029/2020MS002298.
6. Hurrell, James W., M. M. Holland, P. R. Gent, S. Ghan, Jennifer E. Kay, P. J. Kushner, J.-F. Lamarque, et al. "The Community Earth System Model: A Framework for Collaborative Research." Bulletin of the American Meteorological Society 94, no. 9 (September 2013): 1339–60. https://doi.org/10.1175/BAMS-D-12-00121.1.
7. Smirnov, Dimitry, Matthew Newman, Michael A. Alexander, Young-Oh Kwon, and Claude Frankignoul. "Investigating the Local Atmospheric Response to a Realistic Shift in the Oyashio Sea Surface Temperature Front." Journal of Climate 28, no. 3 (February 1, 2015): 1126–47. https://doi.org/10.1175/JCLI-D-14-00285.1.

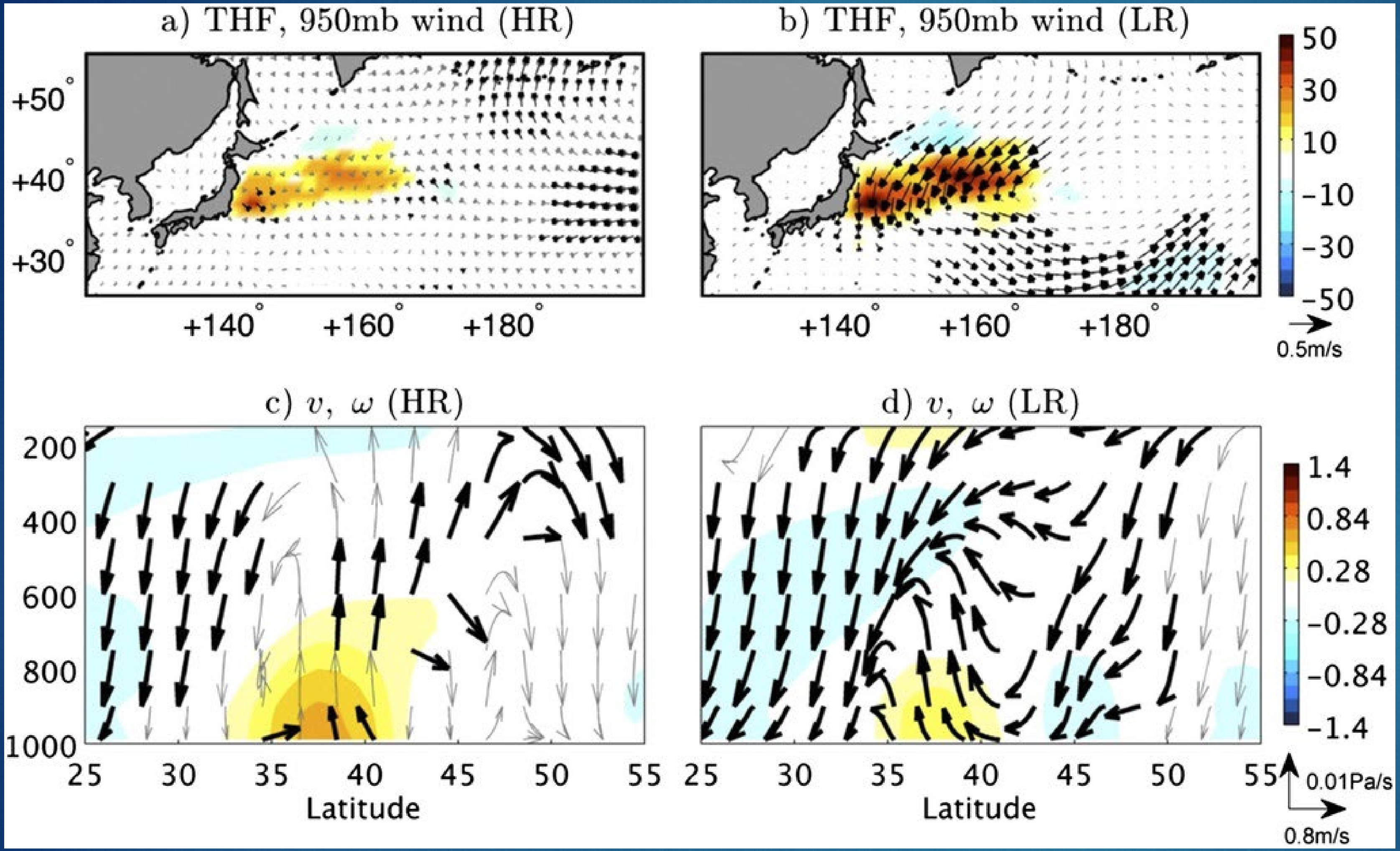

Previous literature shows that sharpening horizontal grid resolution enhances vertical motion in response to a warm SST anomaly

1. Smirnov, Dimitry, Matthew Newman, Michael A. Alexander, Young-Oh Kwon, and Claude Frankignoul. "Investigating the Local Atmospheric Response to a Realistic Shift in the Oyashio Sea Surface Temperature Front." Journal of Climate 28, no. 3 (February 1, 2015): 1126–47. https://doi.org/10.1175/JCLI-D-14-00285.1.

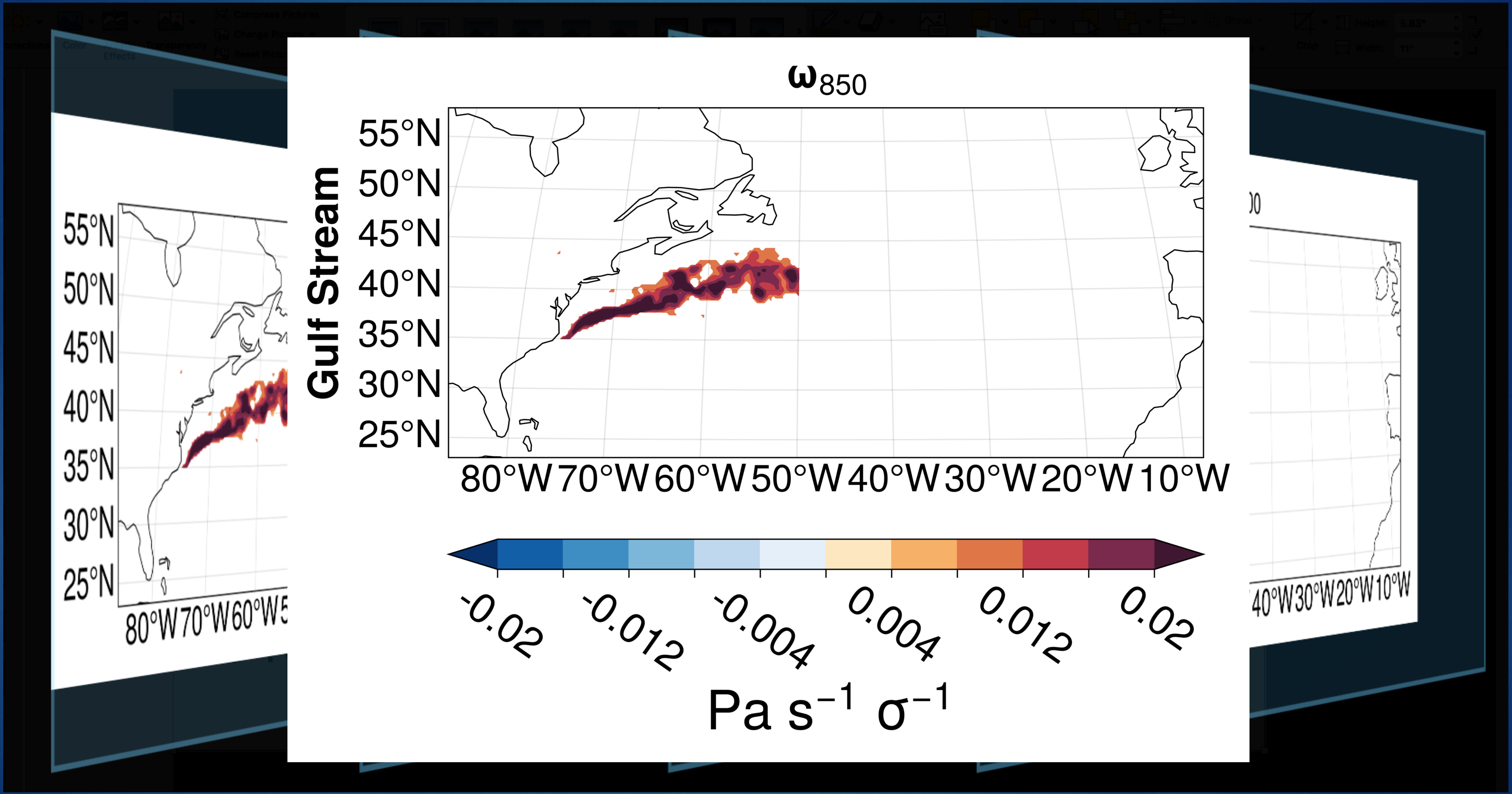
ω850
Gulf Stream
55°N
50°N
45°N
40°N
35°N
30°N
25°N
80°W 70°W 60°W 50°W 40°W 30°W 20°W 10°W
-0.02
-0.012
-0.004
0.004
0.012
0.02
Pa s−1 σ−1

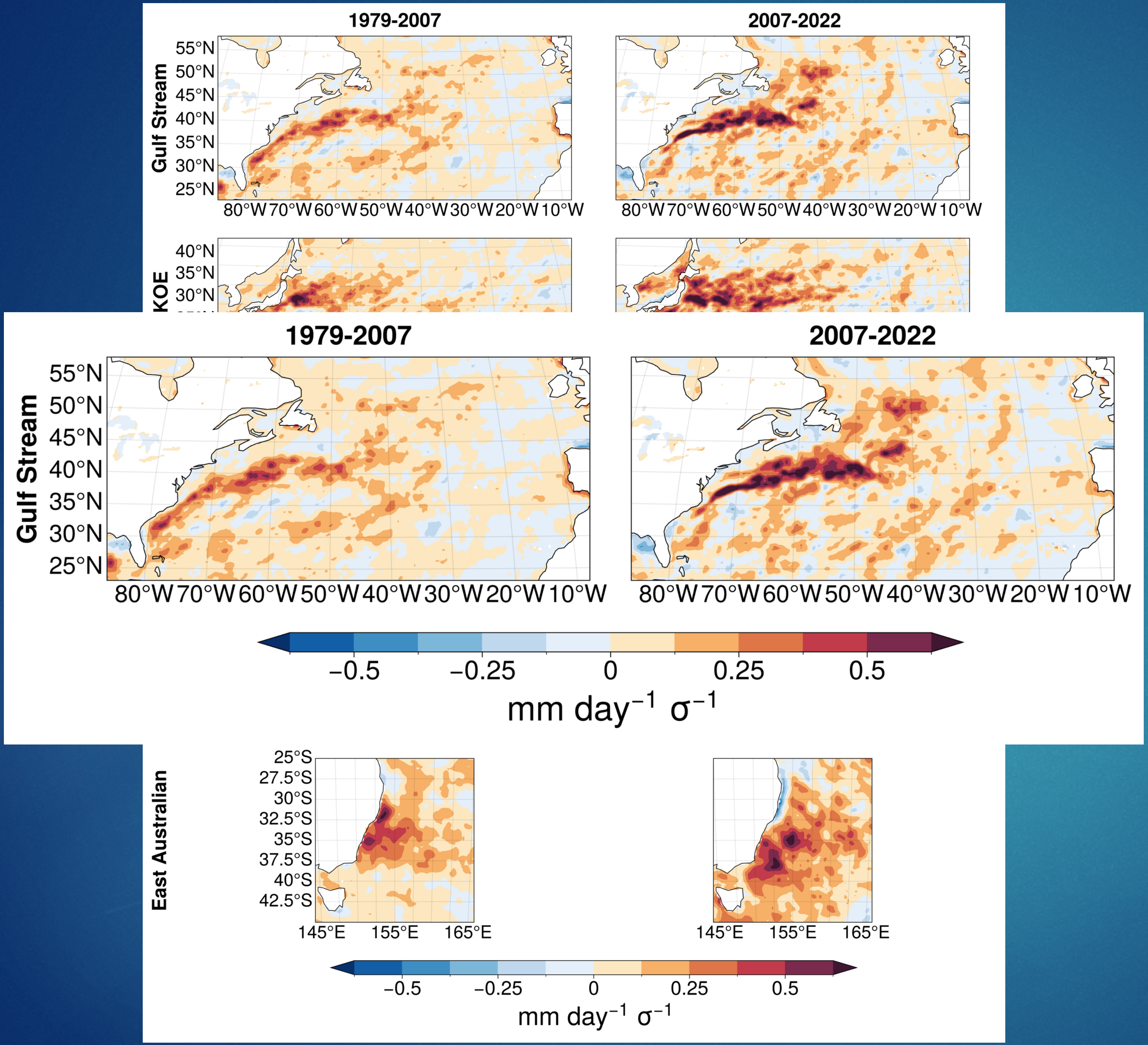

Regression of precipitation anomalies onto standardized SST anomalies

Evidence suggests that fine horizontal resolution in the SST forcing dataset (1/20°) enhances air-sea co-variability

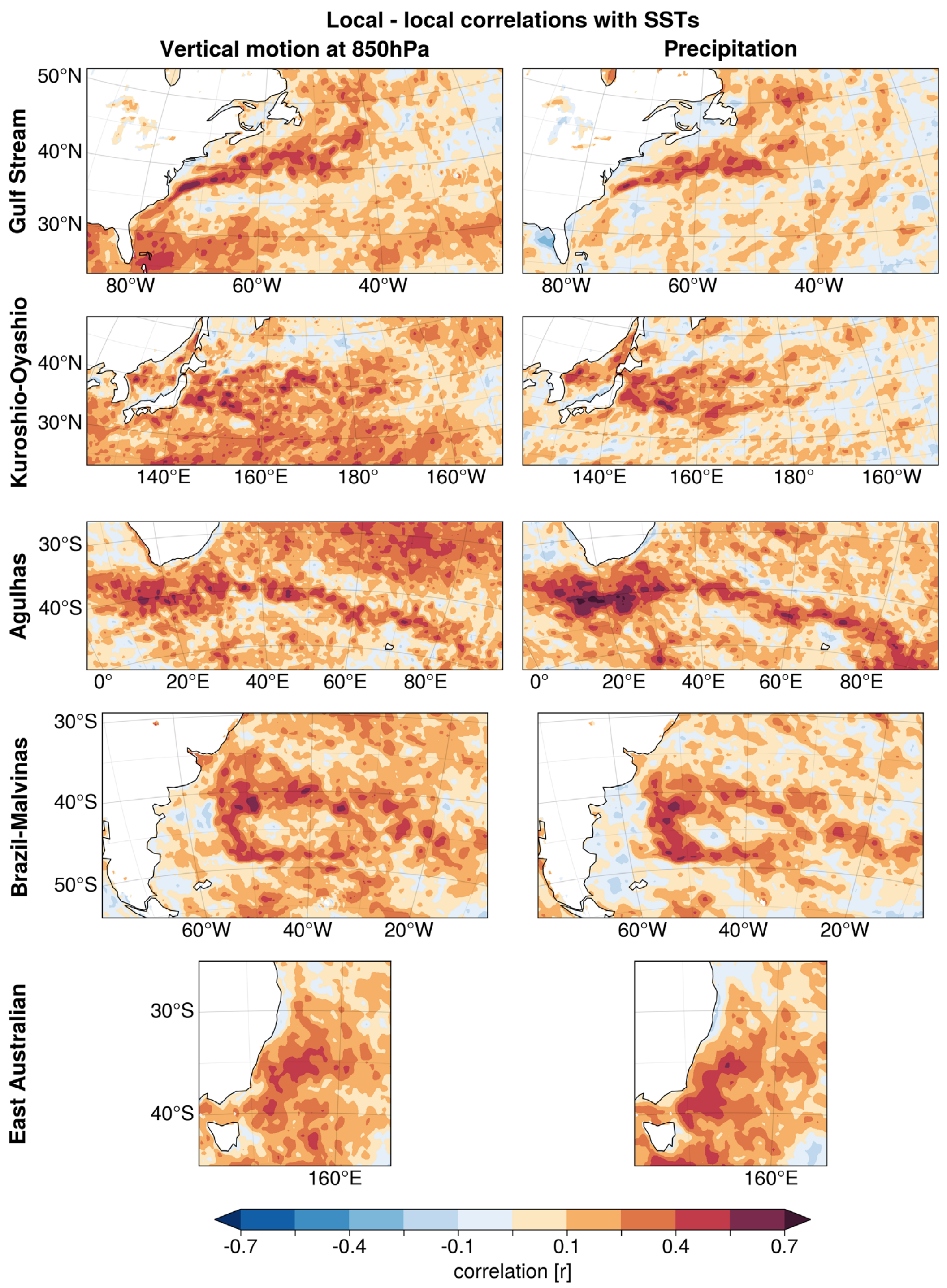
Local - local correlations with SSTs
Vertical motion at 850hPa
Precipitation
Gulf Stream
50°N
40°N
30°N
80°W
60°W
40°W
Kuroshio-Oyashio
40°N
30°N
140°E
160°E
180°
160°W
Agulhas
30°S
40°S
0°
20°E
40°E
60°E
80°E
Brazil-Malvinas
30°S
40°S
50°S
60°W
40°W
20°W
East Australian
30°S
40°S
160°E
-0.7
-0.4
-0.1
0.1
0.4
0.7
correlation [r]

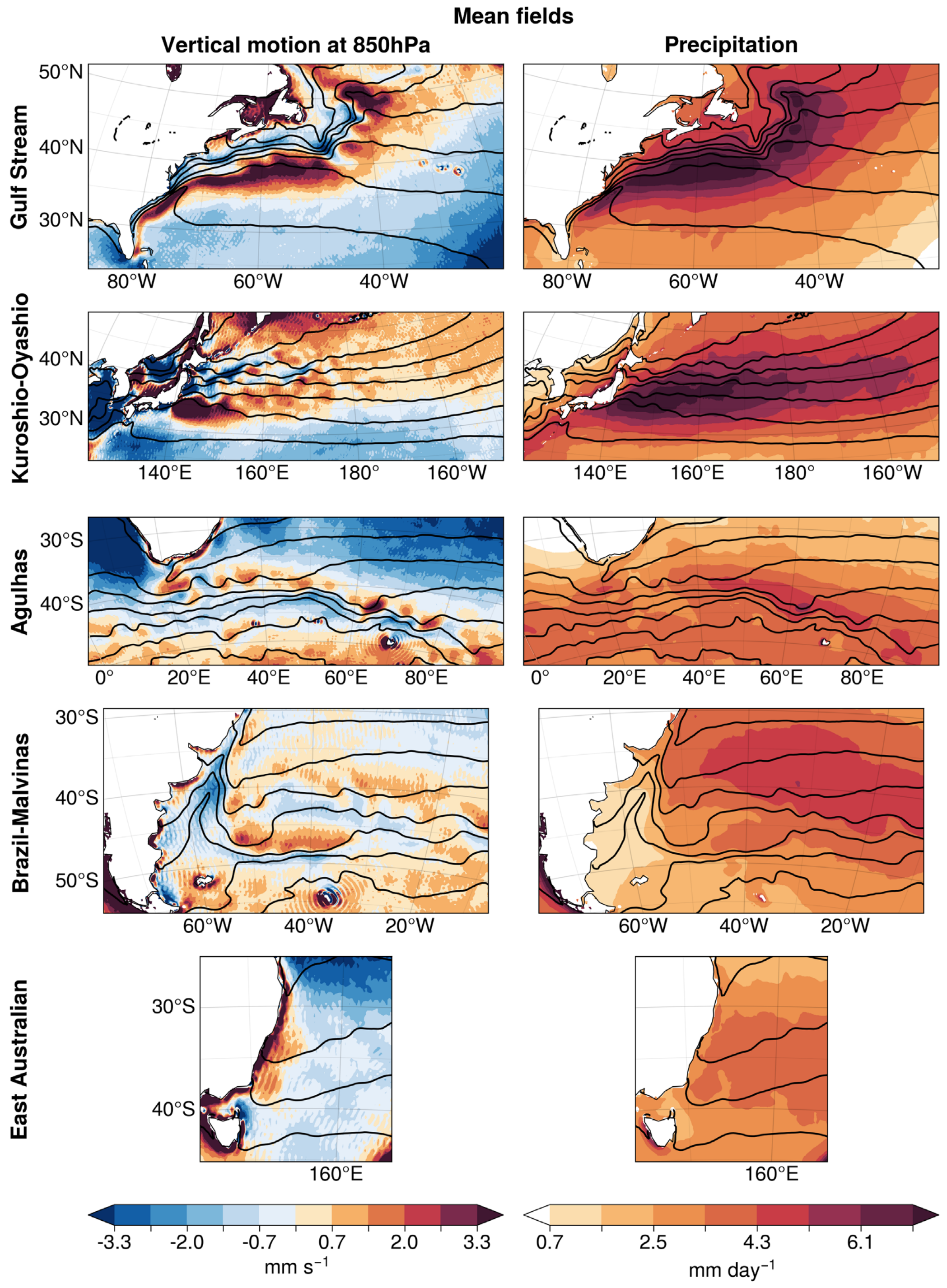
Mean fields
Vertical motion at 850hPa
Precipitation
Gulf Stream
Kuroshio-Oyashio
Agulhas
Brazil-Malvinas
East Australian
50°N
40°N
30°N
80°W
60°W
40°W
140°E
160°E
180°
160°W
30°S
40°S
50°S
0°
20°E
40°E
60°E
80°E
20°W
-3.3 -2.0 -0.7 0.7 2.0 3.3
mm s⁻¹
0.7 2.5 4.3 6.1
mm day⁻¹

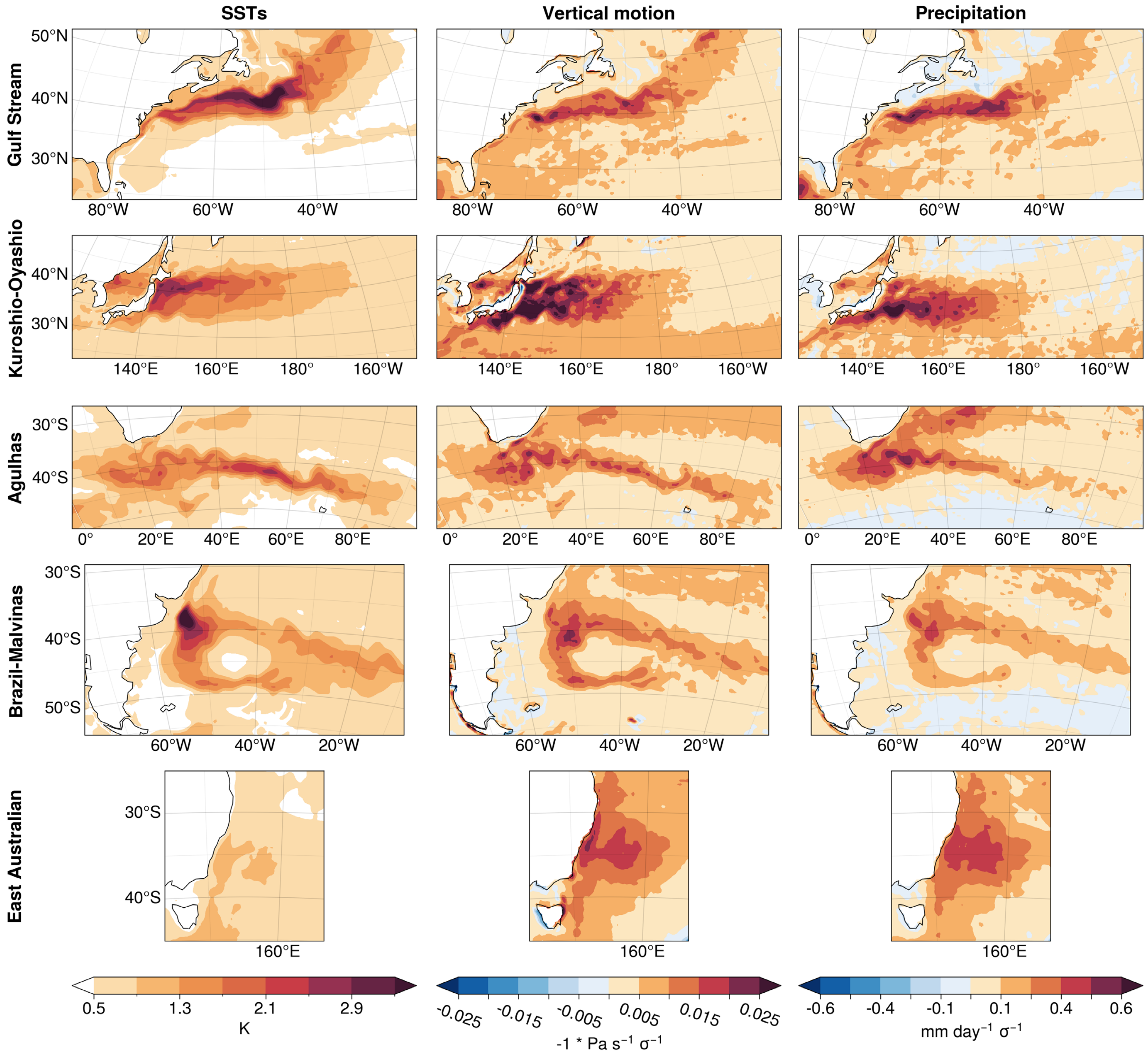
SSTs
Vertical motion
Precipitation
Gulf Stream
Kuroshio-Oyashio
Agulhas
Brazil-Malvinas
East Australian
50°N
40°N
30°N
80°W
60°W
40°W
140°E
160°E
180°
160°W
30°S
40°S
50°S
0°
20°E
40°E
60°E
80°E
20°W
0.5
1.3
2.1
2.9
K
-0.025
-0.015
-0.005
0.005
0.015
0.025
-1 * Pa s^{-1} σ^{-1}
-0.6
-0.4
-0.1
0.1
0.4
0.6
mm day^{-1} σ^{-1}

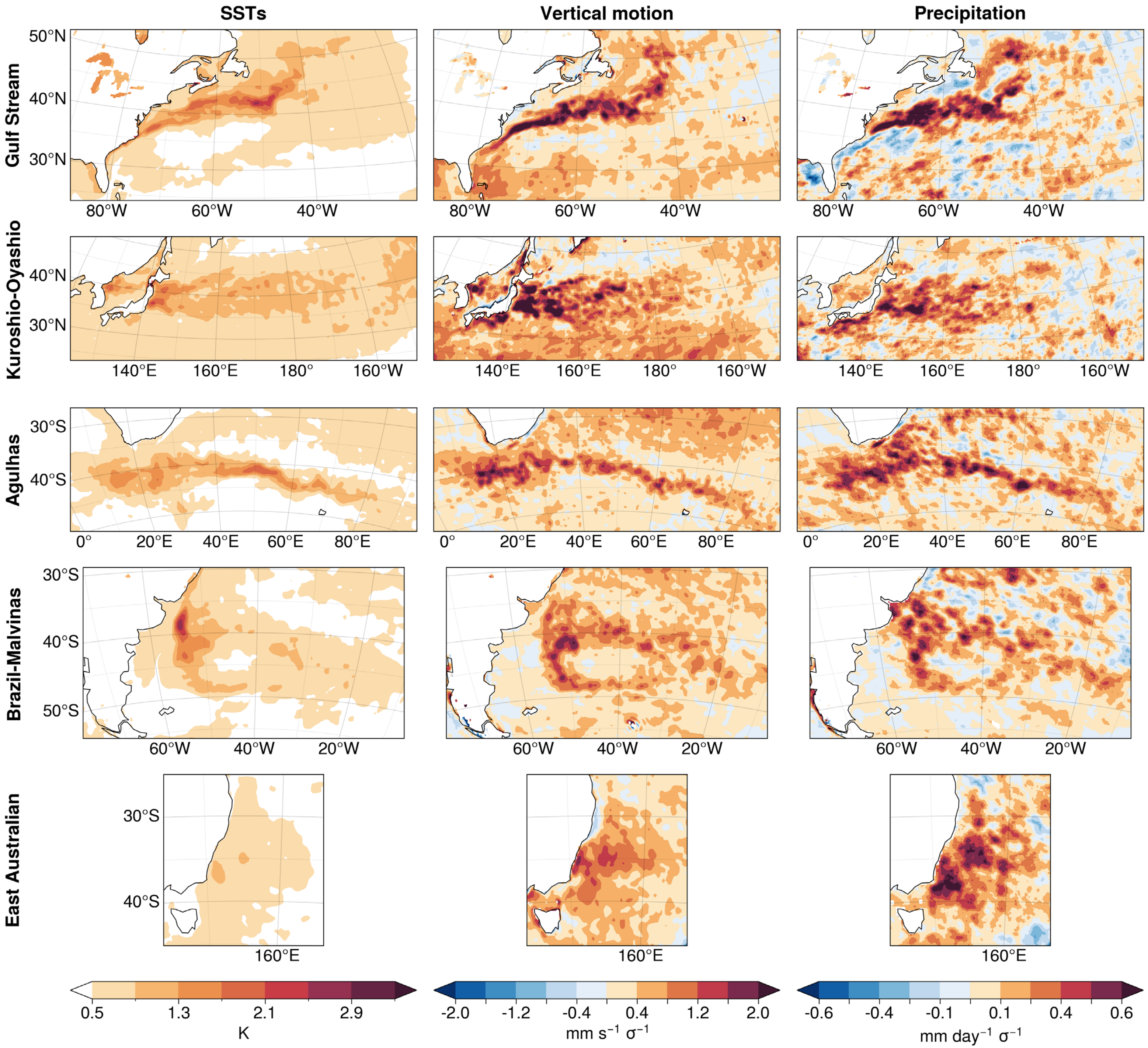
SSTs
Vertical motion
Precipitation
Gulf Stream
Kuroshio-Oyashio
Agulhas
Brazil-Malvinas
East Australian
50°N
40°N
30°N
80°W
60°W
40°W
140°E
160°E
180°
160°W
30°S
40°S
50°S
0°
20°E
40°E
60°E
80°E
60°W
40°W
20°W
160°E
0.5
1.3
2.1
2.9
K
-2.0
-1.2
-0.4
0.4
1.2
2.0
mm s⁻¹ σ⁻¹
-0.6
-0.4
-0.1
0.1
0.4
0.6
mm day⁻¹ σ⁻¹

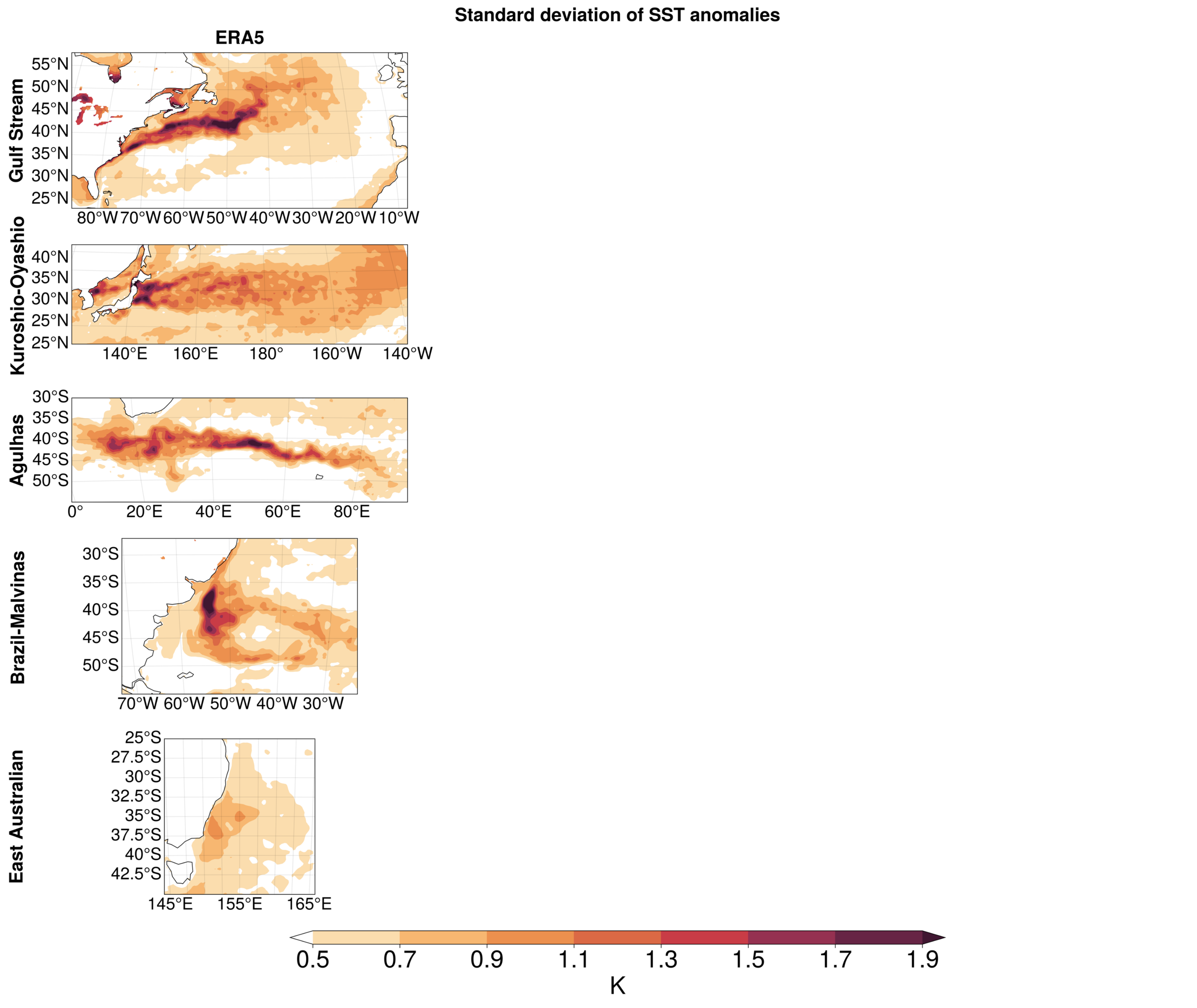

CESM run at 1° resolution underrepresents SST variance in western boundary currents

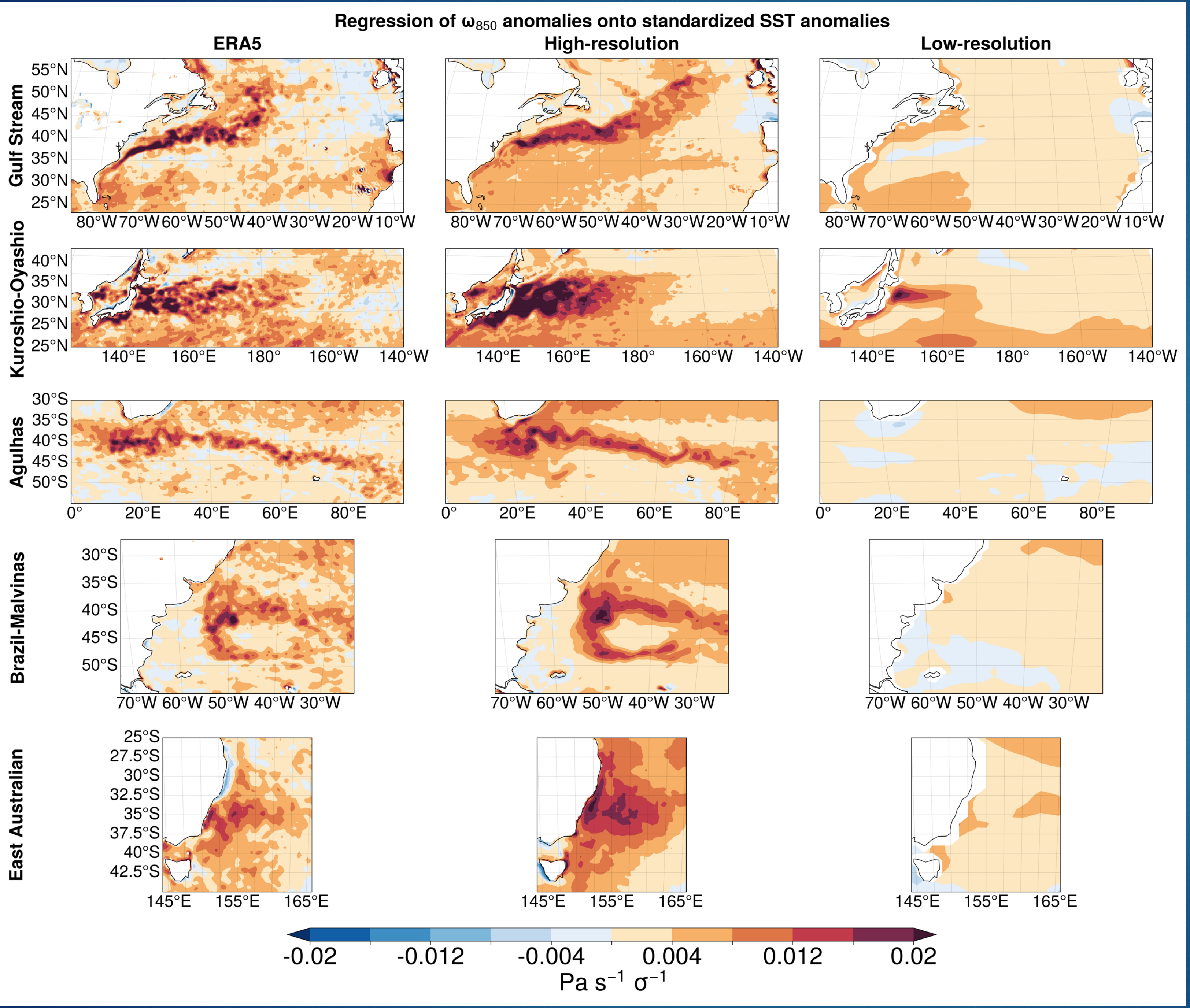

Low resolution CESM shows a near-complete lack of air-sea co-variability in the majority of western boundary currents

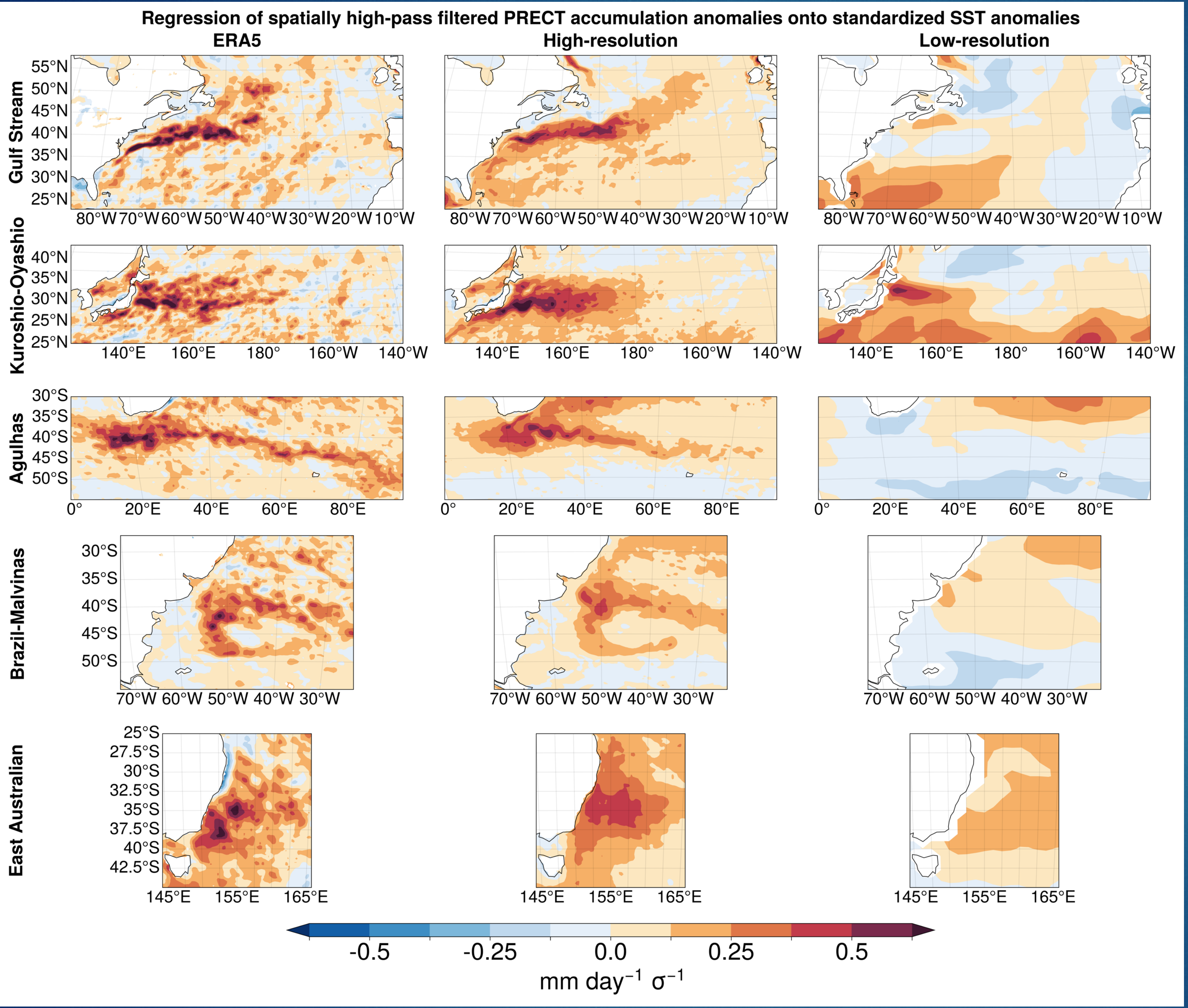

High resolution CESM produces comparable precipitation co-variability to ERA5

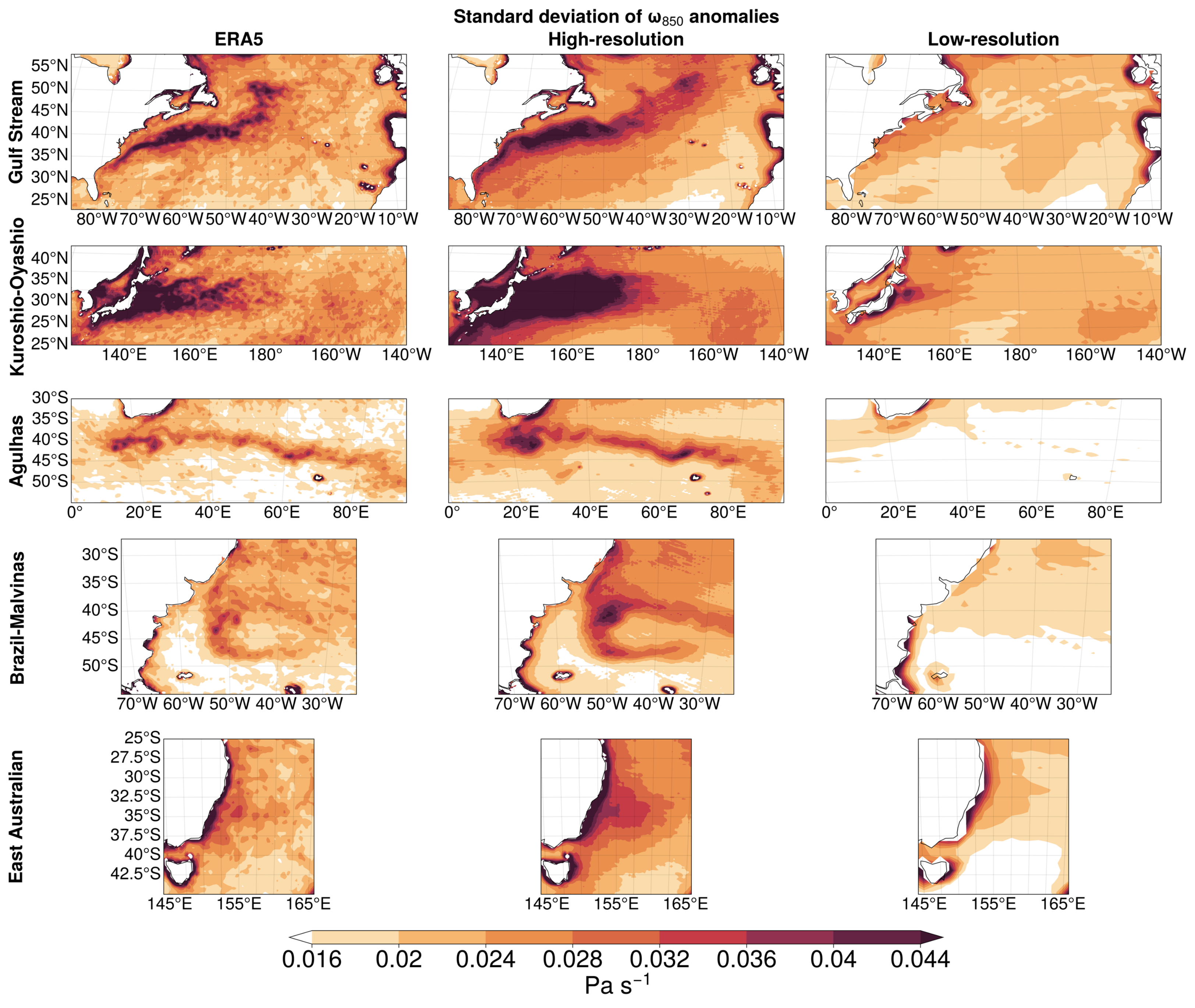

High resolution CESM highlights the strong influence western boundary currents have on the anomalous ω_{850} field

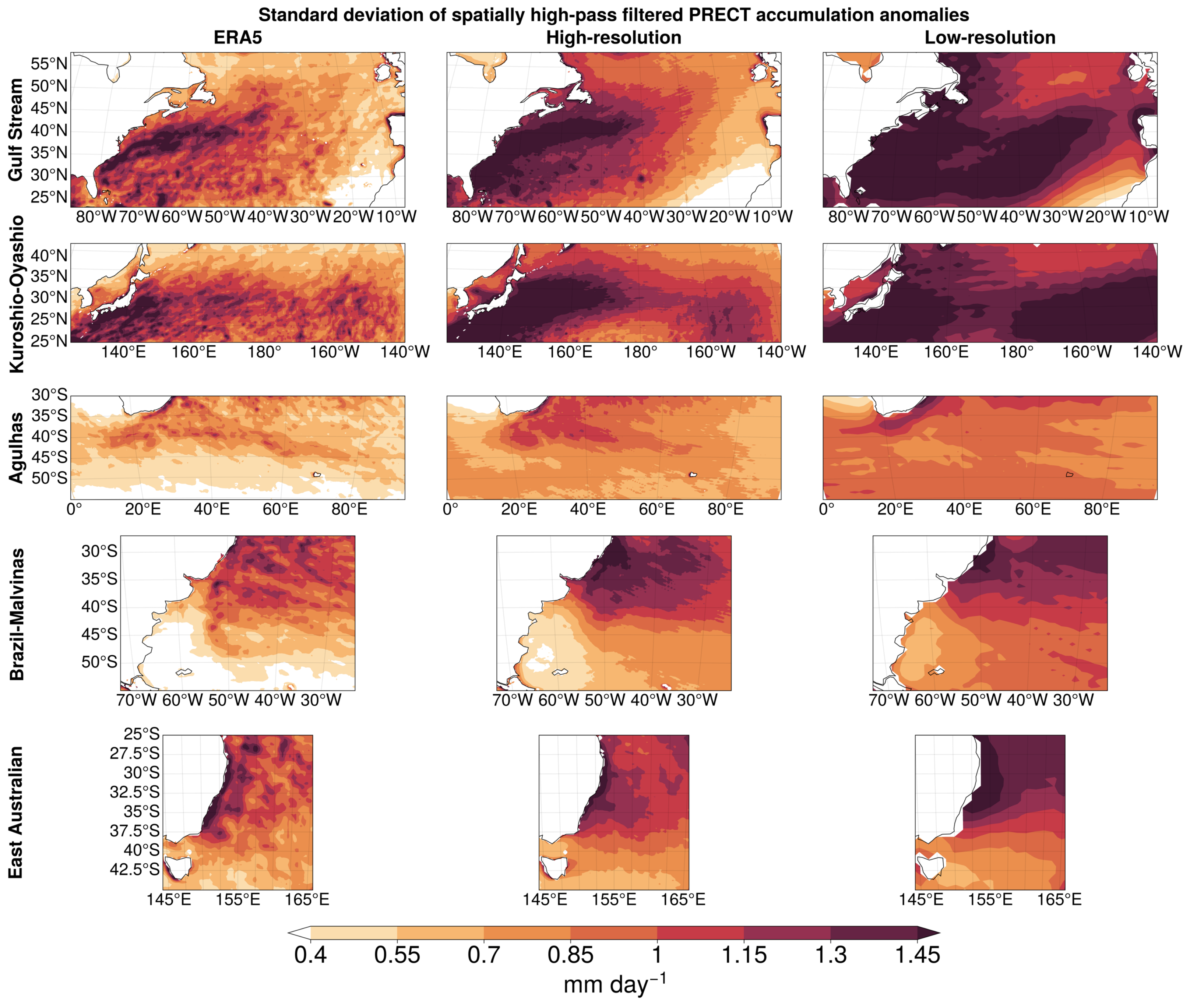

High resolution CESM shows more influence of precipitation by western boundary currents, likely due to longer time length averaging

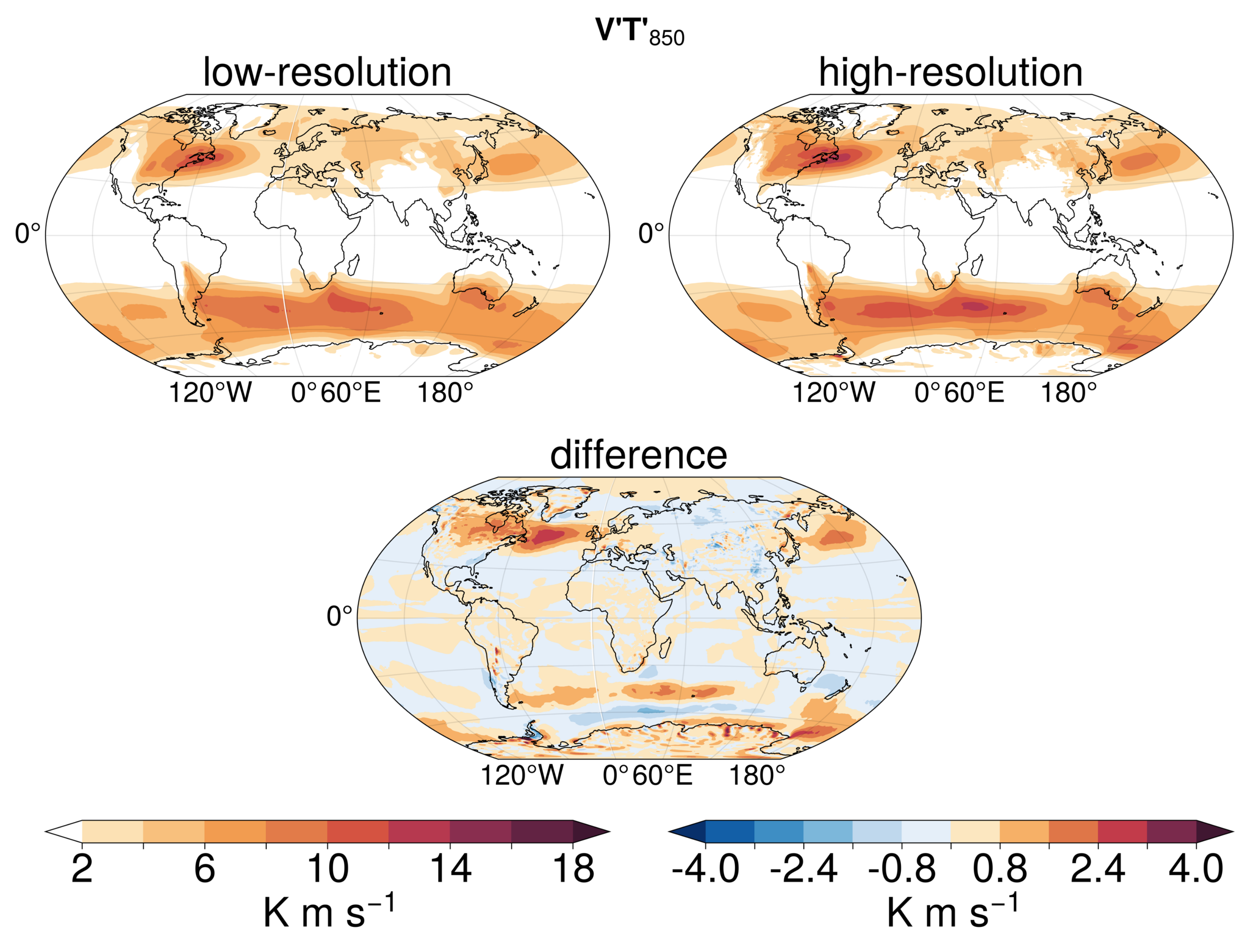

Storm tracks, which are anchored by western boundary currents, are strengthened by increasing horizontal resolution

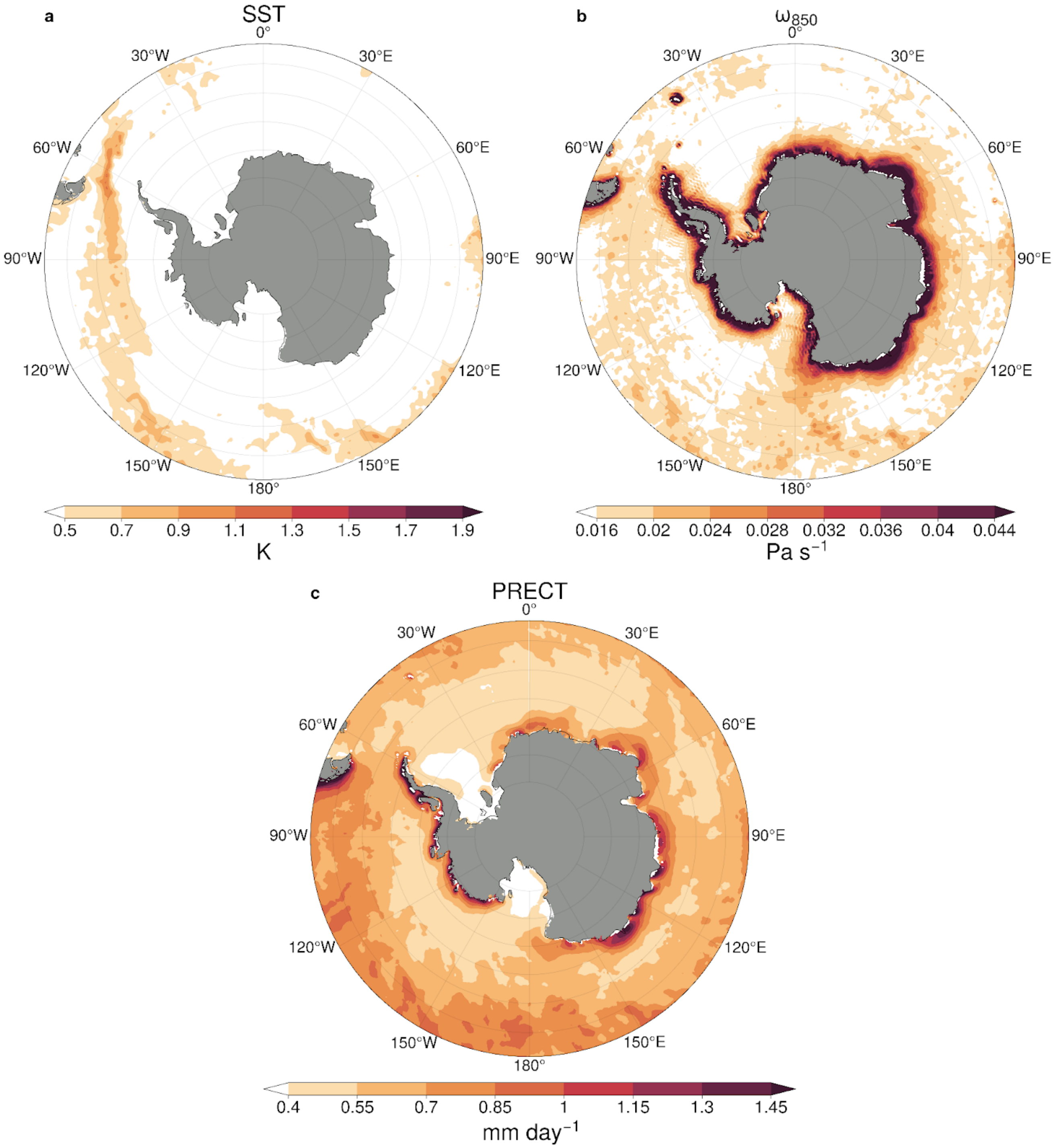

a
SST
0°
30°W
30°E
60°W
60°E
90°W
90°E
120°W
120°E
150°W
150°E
180°
0.5 0.7 0.9 1.1 1.3 1.5 1.7 1.9
K
b
ω850
0°
30°W
30°E
60°W
60°E
90°W
90°E
120°W
120°E
150°W
150°E
180°
0.016 0.02 0.024 0.028 0.032 0.036 0.04 0.044
Pa s−1
c
PRECT
0°
30°W
30°E
60°W
60°E
90°W
90°E
120°W
120°E
150°W
150°E
180°
0.4 0.55 0.7 0.85 1 1.15 1.3 1.45
mm day−1

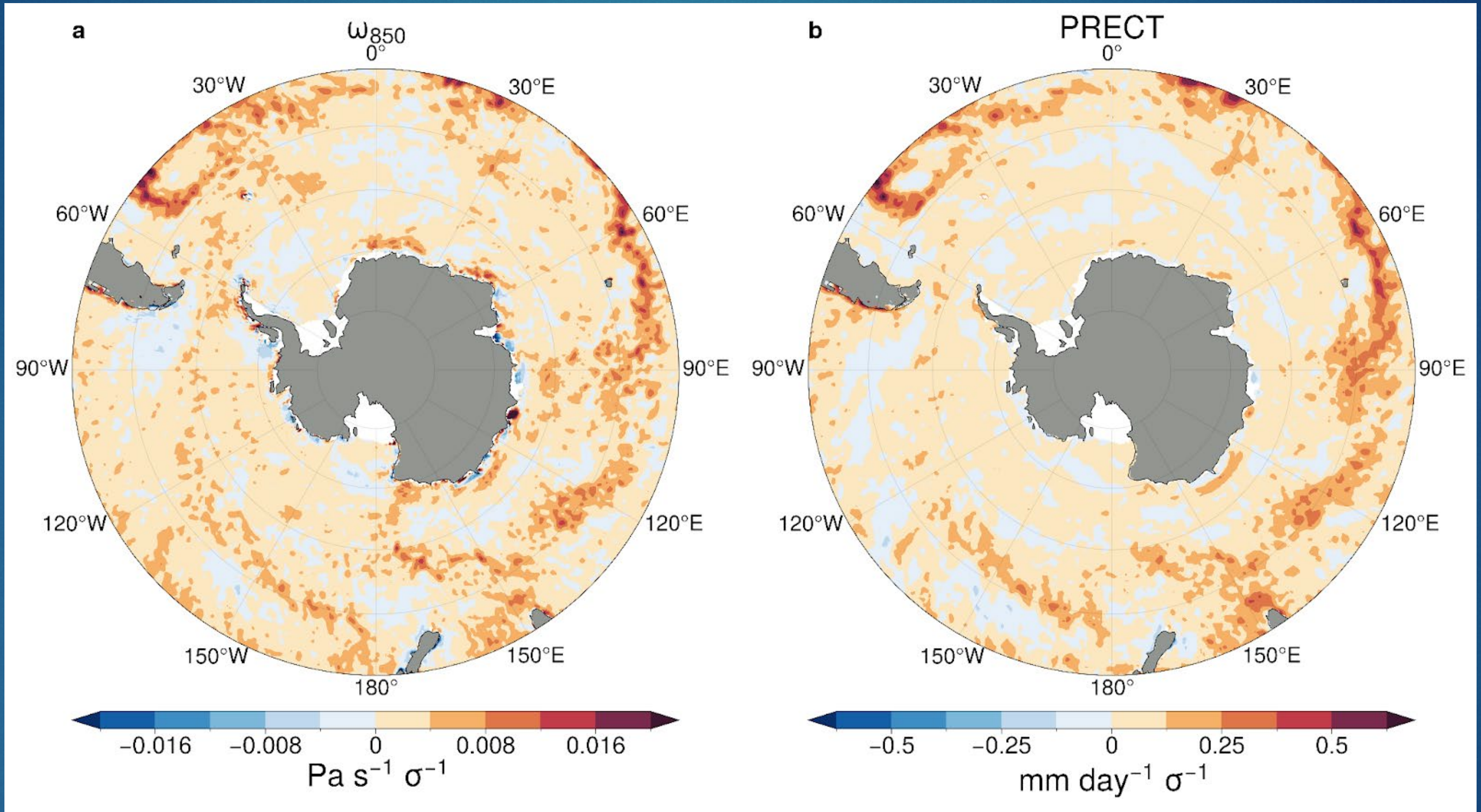
a
ω_{850}
0°
30°W
30°E
60°W
60°E
90°W
90°E
120°W
120°E
150°W
150°E
180°
−0.016
−0.008
0
0.008
0.016
Pa s^{-1} σ^{-1}
b
PRECT
0°
30°W
30°E
60°W
60°E
90°W
90°E
120°W
120°E
150°W
150°E
180°
−0.5
−0.25
0
0.25
0.5
mm day^{-1} σ^{-1}